Nonlinear Saturation Control of an Oscillatory Cantilever Beam Excited Transversely at Its Free End

Ali Kandil, Eman Desoky and Magdy Kamel

***Abstract*—The oscillations of a cantilever beam with transversely energized free under external and parametric excitation forces are studied. When this kind of excitation occurs, external and parametric forces manifest, leading to the intensification of undesired nonlinear oscillations of the beam, especially in resonant states. The nonlinear differential equation that describes the cantilever beam's vibrations can be approximately solved analytically and numerically. To reduce these vibrations, the Nonlinear Saturation Controller (NSC) algorithm is applied using a piezoelectric (PZT) actuator. The PZT actuator is placed throughout the beam's surface to overcome the primary resonance case. Furthermore, the multiple time scales perturbation method is applied to visualize the overall properties of the beam so that the effectiveness of the controller can be assessed. Moreover, the Routh-Hurwitz criterion and Lyapunov's first (indirect) technique are used to verify the stability of the steady-state oscillation amplitude and phase. The cantilever beam bifurcation analysis is presented before and after control, allowing for a comparison of the beam's behavior. Time responses and phase portraits have been used to perform numerical verifications that validate the implemented control method.**

***Keywords*—Cantilever beam; bifurcation; simultaneous resonance; nonlinear saturation controller; phase plane.**

I. INTRODUCTION

In dynamical problems of a beam carrying a concentrated mass at its end or middle may arise. The free vibration characteristics of a uniform or non-uniform beam carrying various concentrated elements are an important problem in this field. Thus, a lot of studies have been published in this area [1-3]. Pratiher and Dwivedy [4] investigated and studied the nonlinear vibration of a cantilever beam with an end mass subjected to an axial force and a periodically shifting magnetic field. The perturbation method is used to solve the system's equation of motion of this cantilever beam that contains both linear and nonlinear parametric excitation terms. The stability and bifurcation at three various resonance cases were investigated and studied numerically. Sadri et al. [5] studied vibrations due to nonlinear motion of forced cantilever beam carrying a midway lumped mass and derived the nonlinear governing equation of the vibrating beam using Euler–Lagrange method. An approximate solution for this problem is obtained using perturbation technique and the stability of each frequency-response curves near the deduced resonance cases are determined numerically. They found frequency response of the cantilever beam is strongly affected by damping and excitation level and by changing the parameters values of the model the transition from the periodic solution to chaos occurred for the mechanical system. Also, Kumar [6] investigated the nonlinear dynamic behavior of cantilever beam response experimentally and numerically under transverse harmonic excitation. The effects of approximation of curvature/inertia nonlinearities and transverse displacement on the nonlinear periodic response of the cantilever beam are obtained. The free vibration and stability analysis of a cantilever beam that was intermittently attached to a tendon and subjected to axial loading are investigated and studied by Ondra and Titurus [7]. The experimental model was developed and tested theoretically with respect to its frequency loading techniques. It has been observed that the system provided frequency reduction for beam-dominated modes and string position skew, which depended on the number and placement of the beam attachment points. In addition, Zhang [8] investigated the non-planar chaotic vibrations of a cantilever beam under the influence of a combination of transverse and axial excitations using perturbation techniques, Galerkin's method, and normal form theory. The effects of important parameters on the stability limits were demonstrated numerically. Sayed et al. [9] studied multiscale turbulence and its numerical solution Vibration analysis and control system simulates the vibrations of a Nonlinear compound beam model. The controller is applied to control one Frequency at primary and parametric resonance where mechanical damage occurs the system is possible. Active control is applied to the system. Multiple metrics the perturbation technique (MSP) is utilized to achieve an estimated analysis solution. Frequency response (FR) is used to provide system stability analysis. Within a variety of bifurcation parameter ranges, the system's dynamic behavior is anticipated. The bifurcation analysis efficiently identifies all stable steady state (point attractor),

Manuscript received [4 July 2024]; revised [17 August 2024]; accepted [12 Sept 2024]. Date of publication [18 Jan 2025]. (*Corresponding author:* Eman Desoky*)*.

Ali Kandil is with Department of Applied and Computational Mathematics, Institute of Basic and Applied Sciences, Egypt-Japan University of Science and Technology (E-JUST), New Borg El-Arab City, 21934, Alexandria, Egypt; and Department of Physics and Engineering Mathematics, Faculty of Electronic Engineering, Menouf, 32952, Menoufia University, Egypt (email: ali.kandil@ejust.edu.eg).

Eman Desoky is with [3]Department of Basic Science, Menoufia Higher Institute of Engineering and Technology, El-Bagour, 32821, Egypt; (email: emandesoky51@gmail.com)

Magdy Kamel is with Department of Physics and Engineering Mathematics, Faculty of Electronic Engineering, Menouf, 32952, Menoufia University, Egypt (email: dr_magdi_kamel@yahoo.com)

periodic stable attractors, unstable steady state, and periodic unstable attractors. Omara et al. [10] investigated nonlinear vibration control of a horizontally supported rotor system, which is governed by two coupled second-order differential equations containing quadratic and cubic nonlinearities. The system is based on the proposed control strategy and the entire system, and the results obtained showed that the proposed control method can mitigate unwanted rotor vibrations near zero regardless of the amplitude. Additionally, an 8-pole active magnetic bearing is used as the active actuator through which the control signal will be applied to the rotor.

Micro-electromechanical systems (MEMS) are devices and technologies that have evolved from the microelectronics industry. MEMS resonators composed mainly of micro beams are the main building block of many MEMS sensors and actuators that are used in variety of applications such as mass sensors, temperature sensors, force and acceleration sensors. These MEMS resonators are excited using different types of forces, such as piezoelectric, thermal and electrostatic [11-14]. Przybylski and Gasiorski [15] studied the theoretical and experimental investigations into nonlinear flexural vibrations of a structure composed of a host beam with piezoelectric ceramic actuators symmetrically bonded to its top and bottom surfaces. The analytical model for describing flexural vibration of a beam under both the external load and piezoelectric actuation is based on the Euler–Bernoulli beam. They created a prestressed which can stabilize the structure when the external compressive force appears by applying voltage to piezoelectric actuators. The solution of the beam system is obtained by applying Lindstedt-Poincare perturbation method. Latalski and Warminski [16] analyzed and studied a revolving structure made up of a hub and a laminate cantilever beam with embedded nonlinear piezoelectric layers and thin walls. The author proposed a nonlinear analytical model of a piezoelectric material embedded onto beam walls, which is represented by mutually coupled nonlinear equations of motion, using higher-order constitutive relations with regard to the electric field variable. Plots of the appropriate frequency response and bifurcation diagrams are used to illustrate the effects of hub inertia, excitation amplitude, and mean rotating speed on system dynamics. Finally Ebrahimi et al. [17] investigated and studied a nonlinear dynamical modeling of smart graphene/piezoelectric composite nanoplates subjected to dual frequency excitation. The multiple time scales method is applied to solve nonlinear problem and to study the modulation equation under sub-harmonic and super-harmonic stimulation. The obtained results showed that dual frequency excitation can intensify the nonlinear frequency response and the electric voltage as well as external excitation plays an important role in resonance phenomenon.

Moreover, many authors studied different vibration controls to suppress the vibration of the structure beams [18-23]. For cantilever beams the favorite controllers such as: velocity feedback control, nonlinear saturation controller (NSC), time-delay feedback control and positive position feedback control are appropriate to eliminate system vibration and enhance the bandwidth of the amplitude beam. Liu et al. [24] investigated and studied a suspended arm beam carrying a lumped mass under a harmonic excitation force. The authors applied the perturbation technique to derive the frequency equations and studied the stability of the vibration system near the fundamental, superharmonic and subharmonic resonance states. They also applied time delay feedback controller to enhance the stability and suppress the nonlinear vibration of the dynamical system. Also, Hamed et al. [25], studied the nonlinear vibrations of a cantilever beam system carrying an intermediate lumped mass. They applied multi scale method to obtain an approximate solution of the vibrating system and to derive the response of amplitudes and phases to study the stability of the vibration system near the worst resonance case and to study bifurcation of the oscillating system. Finally, the suppression of vibrating system is obtained when the modified positive position feedback (MPPF) approach is applied and they found the optimized choice of control parameters can be useful in controlling vibrations. Finally, Amer et al. [26] studied how to suppress the vibrations of a cantilever beam excited by an external force using four different types of controllers, namely linear velocity feedback controller, cubic velocity feedback controller, nonlinear saturation controller, and positive local feedback controller. They applied the multi scale perturbation method to obtain the approximate solution of the beam equation and derived the response of amplitudes and phases equations to investigate the stability of the vibrating beam near the worst case resonance. The researchers found that the positive local feedback controller is a suitable controller for suppressing the vibrations of a cantilever beam.

This study presents a model of a nonlinear cantilever beam under the influence of external and parametric stimulating forces. A nonlinear saturation controller (NSC) is applied to suppress the resulting nonlinear vibrations. The multi scale method [27,28] is applied to derive the frequency response equations and obtain the approximate analytical solution of the oscillating system. In addition, the stability of the equilibrium solutions near the synchronous intrinsic and fundamental resonance condition is investigated and evaluated. The approximate numerical solution is obtained using numerical integration through the Rung-Kutta technique. In addition, the effects of changing all the parameters on the frequency response curves of the oscillating beam are investigated. Finally, some tips regarding the applied control technique are provided, along with a summary of its advantages and limitations.

II. MATHEMATICAL ANALYSIS ON THE CANTILEVER BEAM'S MOTION

The schematic diagram of the cantilever beam is displayed in Figure (1). The governing equation of motion of the vibrating beam system was studied before in Ref [8]. Utilizing an NSC algorithm, it can be coupled to the beam's equation of motion to have the following

$$\ddot{\upsilon}+\bar{c}\dot{\upsilon}+\beta_y\upsilon^{(4)}+F_1\cos(\Omega_1 \mathrm{t})\upsilon''$$
$$=-\beta_y\left[\upsilon'(\upsilon'\upsilon'')'\right]'$$
$$-\frac{1}{2}\left[\upsilon'\int_1^s\frac{d^2}{dt^2}\left\{\int_0^s\upsilon'^2ds\right\}ds\right]'$$
$$-F_1\cos(\Omega_1 \mathrm{t})\left[\upsilon'\upsilon'^2\right]'$$
$$+F_2(\mathrm{s})\cos(\Omega_2 \mathrm{t})+kv^2 \quad (1)$$

Under coupled parametric and driving excitations, we construct a two-degree-of-freedom nonlinear system in the following analysis by using the Galerkin approach to Equation (1). For the cantilever beam, the planar flexural mode is regarded as

$$v(s,t)=y(t)G(s) \quad (4)$$

$$\ddot{y}G+\bar{c}\dot{y}G+\beta_y yG^{(4)}+F_1\cos(\Omega_1 \mathrm{t})\mathrm{y}\mathrm{G}''$$
$$=-\beta_y\left[\mathrm{y}\mathrm{G}'(\mathrm{y}\mathrm{G}'\mathrm{y}\mathrm{G}'')'\right]'$$
$$-\frac{1}{2}\left[\mathrm{y}\mathrm{G}'\int_1^s\frac{d^2}{dt^2}\left\{\int_0^s(\mathrm{y}\mathrm{G}')^2ds\right\}ds\right]'$$
$$-F_1\cos(\Omega_1 \mathrm{t})\left[\mathrm{y}\mathrm{G}'(\mathrm{y}\mathrm{G}')^2\right]'$$
$$+F_2(\mathrm{s})\cos(\Omega_2 \mathrm{t})+kv^2 \quad (5)$$

where the position s denotes the curve coordinate along the elastic axis before deformation and the function $G(s)$ denotes the linear mode of transverse free vibration. It takes the following form

$$G(\mathrm{s})=\cosh(\mathrm{rs})-\cos(\mathrm{rs})$$
$$-\left[\left(\cosh(\mathrm{r})+\cos(\mathrm{r})/(\sinh(\mathrm{r})+\sin(\mathrm{r}))\right)\right]$$
$$*\left[\sinh(\mathrm{rs})-\sin(\mathrm{rs})\right] \quad (6)$$

The following ordinary differential equation is satisfied by the linear mode $G(s)$

$$G^{(4)}-r^4G=0 \quad (7)$$

subjected to

$$G(0)=\mathrm{G}'(0)=\mathrm{G}''(1)=\mathrm{G}'''(1)=0 \quad (8)$$

The typical equation that determines the r in Equation (7) is

$$\cosh(\mathrm{r})\cos(\mathrm{r})+1=0 \quad (9)$$

Equation (5) is multiplied by G multiplied and is integrated w.r.t. s from 0 to 1 to obtain the following

$$\ddot{v}+\mu\dot{v}+\beta_c v=\gamma_2\upsilon v \quad (2)$$

with the normalized boundary conditions:

$$\upsilon(0,\mathrm{t})=\upsilon'(0,\mathrm{t})=\upsilon''(1,\mathrm{t})=\upsilon'''(1,\mathrm{t})=0 \quad (3)$$

$$\ddot{y}\int_0^1G^2ds+\bar{c}\dot{y}\int_0^1G^2ds+\beta_y\int_0^1GyG^{(4)}ds$$
$$+F_1\cos(\Omega_1 \mathrm{t})\mathrm{y}\int_0^1G\mathrm{G}''ds$$
$$=-\beta_y y^3\int_0^1G\left[\mathrm{G}'(\mathrm{G}'\mathrm{G}'')'\right]'ds$$
$$-\frac{1}{2}y^3\int_0^1G\left[\mathrm{y}\mathrm{G}'\int_1^s\frac{d^2}{dt^2}\left\{\int_0^s(\mathrm{y}\mathrm{G}')^2ds\right\}ds\right]'ds$$
$$-y^3F_1\cos(\Omega_1 \mathrm{t})\int_0^1\mathrm{G}\left[\mathrm{G}'(\mathrm{G}')^2\right]'ds$$
$$+\cos(\Omega_2 \mathrm{t})\int_0^1GF_2(\mathrm{s})ds+kv^2\int_0^1G^2ds \quad (10)$$

Under coupled parametric and driving excitations, a nonlinear system with two degrees of freedom is formed as

$$\ddot{y}+c\dot{y}+\beta_y y-2\alpha_1F_1\cos(\Omega_1 \mathrm{t})\mathrm{y}+\alpha_2y(y\ddot{y}+\dot{y}^2)$$
$$+\alpha_3\beta_y y^3-2\bar{F}_1\cos(\Omega_1 \mathrm{t})\mathrm{y}^3=f_1\cos(\Omega_2 \mathrm{t})+\gamma_1v^2 \quad (11)$$

$$\ddot{v}+\mu\dot{v}+\beta_c v=\gamma_2 y v \quad (12)$$

where the dot denotes the differentiation w.r.t. $\tilde{\tau}=r^2t$, and the parameters above are given by

$$c=\frac{\bar{c}}{r^2},\ \alpha_1=\frac{-1}{r^4}\int_0^1GG''ds,$$

$$\alpha_2=\int_0^1G\left[G'\int_1^s\int_0^sG'^2dsds\right]'ds,\ \gamma_1=\frac{k}{r^2}$$

$$\alpha_3=\frac{1}{r^4}\int_0^1G\left[G'(G'G'')'\right]'ds,\ f_1=\frac{1}{r^4}\int_0^1GF_2ds$$

and $\bar{F}_1=\frac{-F_1}{2r^4}\int_0^1G(\mathrm{G}'^3)'ds$ (13)

Appropriate scaled parameters for using the multiple scales approach are introduced as follows

$$\alpha_1\to\varepsilon\alpha_1,\ \alpha_2\to\varepsilon\alpha_2,\alpha_3\to\varepsilon\alpha_3,\ \bar{F}_1\to\varepsilon\bar{F}_1,$$
$$c\to\varepsilon c,f_1\to\varepsilon f_1,\gamma_1\to\varepsilon\gamma_1,\gamma_2\to\varepsilon\gamma_2,$$
$$\mu\to\varepsilon\mu \quad (14)$$

where $0<\varepsilon\ll1$ is a small perturbation parameter. In addition, β_y and β_c can be replaced by ω^2 and ω_c^2 in the next stage of analysis. Inserting Equation (14) into (11) and (12) yields

$$\ddot{y}+\varepsilon c\dot{y}+\omega^2 y-2\varepsilon\alpha_1 F_1\cos(\Omega_1 t)y+\varepsilon\alpha_3\omega^2 y^3 +\varepsilon\alpha_2 y(y\ddot{y}+\dot{y}^2)-2\varepsilon\bar{F}_1\cos(\Omega_1 t)y^3 = \varepsilon f_1\cos(\Omega_2 t)+\varepsilon\gamma_1 v^2 \quad (15)$$

$$\ddot{v}+\varepsilon\mu\dot{v}+\omega_c^2 v=\varepsilon\gamma_2 y v \quad (16)$$

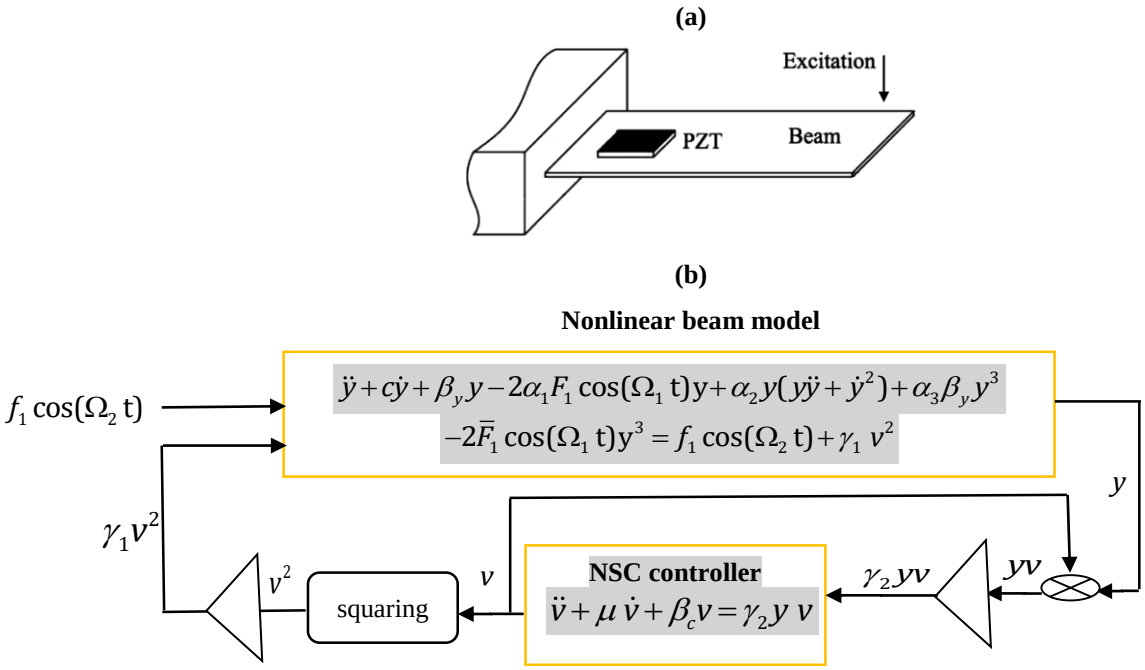

Figure 1. (a) Cantilever beam with piezoelectric configuration, (b) the controlled cantilever beam block diagram.

The multiple scales approach [27, 28] is utilized to seek a first-order uniform solution to equations (15) and (16) as

$$y(t,\varepsilon)=y_0(T_0,T_1)+\varepsilon y_1(T_0,T_1)+\cdots \quad (17.a)$$

$$v(t,\varepsilon)=v_0(T_0,T_1)+\varepsilon v_1(T_0,T_1)+\cdots \quad (17.b)$$

where $T_0=t$ and $T_1=\varepsilon t$ are the adopted time scales. The time derivatives in terms of T_0 and T_1, will take the form

$$\frac{d}{dt}=\frac{\partial}{\partial T_0}\frac{\partial T_0}{\partial t}+\frac{\partial}{\partial T_1}\frac{\partial T_1}{\partial t}=D_0+\varepsilon D_1 \quad (18.a)$$

$$\frac{d^2}{dt^2}=D_0^2+2\varepsilon D_0 D_1 \quad (18.b)$$

The following can be obtained by equalizing the coefficients of ε on both sides and substituting Equations (17) and (18) into (15) and (16)

ε^0 :

$$D_0^2 y_0+\omega^2 y_0=0 \quad (19.a)$$

$$D_0^2 v_0+\omega_c^2 v_0=0 \quad (19.b)$$

and,

ε^1 : (20.a)

$$D_0^2 y_1+\omega^2 y_1=-2D_0D_1y_0-cD_0y_0+2\alpha_1F_1\cos(\Omega_1 t)y_0 -\alpha_2 y_0^2 D_0^2 y_0-\alpha_2 y_0(D_0 y_0)^2-\alpha_3\omega^2 y_0^3 +2\bar{F}_1\cos(\Omega_1 t)y_0^3+f_1\cos(\Omega_2 t)+\gamma_1 v_0^2$$

$$D_0^2 v_1+\omega_c^2 v_1=-2D_0D_1v_0-\mu D_0 v_0+\gamma_2 y_0 v_0 \quad (20.b)$$

Equation (19) has a solution in the form

$$y_0=Ae^{i\omega T_0}+\bar{A}e^{-i\omega T_0} \quad (21.a)$$

$$v_0=A_1e^{i\omega_c T_0}+\bar{A}_1e^{-i\omega_c T_0} \quad (21.b)$$

where the over-barred terms denote the complex conjugate of the preceding terms. By substituting Equation (21) into Equation (20), the following are obtained

$$D_0^2 y_1 + \omega^2 y_1 = -2\left[i\omega A' e^{i\omega T_0} \right] - c\left[i\omega A e^{i\omega T_0} \right] + \alpha_1 F_1 A\left[e^{i(\omega+\Omega_1)T_0} + e^{i(\omega-\Omega_1)T_0} \right] - \alpha_2 \omega^2 \left[A^3 e^{3i\omega T_0} + 3\bar{A} A^2 e^{i\omega T_0} \right] + \bar{F}_1 A^3 e^{i(3\omega+\Omega_1)T_0} + 3\bar{F}_1 A^2 \bar{A} e^{i(\omega+\Omega_1)T_0} + \alpha_2 \omega^2 \left[A^3 e^{3i\omega T_0} - A^2 \bar{A} e^{i\omega T_0} \right] - 3\alpha_3 \omega^2 A^2 \bar{A} e^{i\omega T_0} - \alpha_3 \omega^2 A^3 e^{3i\omega T_0} + \gamma_1 \left[A_1^2 e^{2i\omega_c T_0} + 2A_1 \bar{A}_1 \right] + \frac{1}{2} f_1 e^{i\Omega_2 T_0} + c.c. \quad (22.a)$$

$$D_0^2 v_1 + \omega_c^2 v_1 = -2D_1\left[i\omega_c A_1 e^{i\omega_c T_0} \right] - \mu i\omega_c A_1 e^{i\omega_c T_0} + \gamma_2 [A e^{i\omega T_0} A_1 e^{i\omega_c T_0} + A e^{i\omega T_0} \bar{A}_1 e^{-i\omega_c T_0}] + c.c. \quad (22.b)$$

The worst resonance case that was deduced form Equations (23), is the simultaneous resonance ($\Omega_2 = \omega$, $\omega_c = \omega$). By using the detuning parameters σ_1 and σ_2, the proximity of the simultaneous resonance can be quantitatively defined as

$$\Omega_2 = \omega + \varepsilon\sigma_1 \quad \text{and} \quad 2\omega_c = \omega + \varepsilon\sigma_2 \quad (23)$$

Substituting Equations (23) into Equations (22), then eliminating the secular terms for y and v solutions in order to get the following solvability conditions

$$-2i\omega A' - ci\omega A + 2\alpha_2 \omega^2 A^2 \bar{A} - 3\alpha_3 \omega^2 A^2 \bar{A} + \frac{f_1}{2} e^{i\sigma_1 T_1} + \gamma_1 A_1^2 e^{i\sigma_2 T_1} = 0 \quad (24.a)$$

$$-2i\omega_c A_1' - \mu i\omega_c A_1 + \gamma_2 A \bar{A}_1 e^{-i\sigma_2 T_1} = 0 \quad (24.b)$$

It is convenient to express $A(T_1)$ and $A_1(T_1)$ in the complex polar form as

$$A = \frac{a_1}{2} e^{ib_1} \quad \text{and} \quad A_1 = \frac{a_2}{2} e^{ib_2} \quad (25)$$

where a_1, a_2, b_1 and b_2 are real functions of T_1. By inserting Equations (25) into (24), the following can be gained where the real functions of T_1 are a_1, a_2, b_1 and b_2. Equation (25) can be inserted into (24), yielding the following results.

$$-i\omega a_1' + \omega a_1 b_1' - \frac{1}{2} ci\omega a_1 + \frac{1}{4}\alpha_2 \omega^2 a_1^3 - \frac{3}{8}\alpha_3 \omega^2 a_1^3 + \frac{f_1}{2} e^{i(\sigma_1 T_1 - b_1)} + \frac{a_2^2}{4}\gamma_1 e^{i(\sigma_2 T_1 - b_1 + 2b_2)} = 0 \quad (26)$$

$$-i\omega_c a_2' + \omega_c a_2 b_2' - \frac{a_2}{2}\mu i\omega_c + \frac{a_1 a_2}{4}\gamma_2 e^{i(b_1 - 2b_2 - \sigma_2 T_1)} = 0 \quad (27)$$

Separating real and imaginary parts from Equations (26) and (27), we have

$$a_1' = -\frac{1}{2} c a_1 + \frac{f_1}{2\omega}\sin\phi_1 + \frac{a_2^2}{4\omega}\gamma_1 \sin\phi_2 \quad (28.a)$$

$$a_1 b_1' = -\frac{1}{4}\alpha_2 \omega a_1^3 + \frac{3}{8}\alpha_3 \omega a_1^3 - \frac{f_1}{2\omega}\cos\phi_1 - \frac{a_2^2}{4\omega}\gamma_1 \cos\phi_2 \quad (28.b)$$

$$a_2' = -\frac{a_2}{2}\mu - \frac{a_1 a_2}{4\omega_c}\gamma_2 \sin\phi_2 \quad (28.c)$$

$$a_2 b_2' = -\frac{a_1 a_2}{4\omega_c}\gamma_2 \cos\phi_2 \quad (28.d)$$

Where $(\sigma_1 T_1 - b_1) = \phi_1$ and $(\sigma_2 T_1 + 2b_2 - b_1) = \phi_2$ (29)

Substituting the T_1-derivatives of Equations (29) into (28) gives a modified autonomous system of differential equations

$$a_1' = -\frac{1}{2} c a_1 + \frac{f_1}{2\omega}\sin\phi_1 + \frac{a_2^2}{4\omega}\gamma_1 \sin\phi_2 \quad (30.a)$$

$$\phi_1' = \sigma_1 + \frac{1}{4}\alpha_2 \omega a_1^2 - \frac{3}{8}\alpha_3 \omega a_1^2 + \frac{f_1}{2\omega a_1}\cos\phi_1 + \frac{a_2^2}{4\omega a_1}\gamma_1 \cos\phi_2 \quad (30.b)$$

$$a_2' = -\frac{a_2}{2}\mu - \frac{a_1 a_2}{4\omega_c}\gamma_2 \sin\phi_2 \quad (30.c)$$

$$\phi_2' = \sigma_2 - \frac{a_1}{2\omega_c}\gamma_2 \cos\phi_2 + \frac{1}{4}\alpha_2 \omega a_1^2 - \frac{3}{8}\alpha_3 \omega a_1^2 + \frac{f_1}{2\omega a_1}\cos\phi_1 + \frac{a_2^2}{4\omega a_1}\gamma_1 \cos\phi_2 \quad (30.d)$$

The above equations govern the fluctuations in the beam's motion amplitude and phase that characterize its output response.

III. STABILITY TEST VIA JACOBIAN MATRIX AND ROUTH-HURWITZ CRITERION

For the steady state solutions we have $a_1' = a_2' = \phi_1' = \phi_2' = 0$, and Equations (30) become in the form:

$$\frac{f_1}{2\omega}\sin\phi_1 = \frac{1}{2} c a_1 + \frac{\omega_c}{2\omega\gamma_2 a_1}\gamma_1 \mu a_2^2 \quad (31.a)$$

$$\frac{f_1}{2\omega}\cos\phi_1 = -a_1\sigma_1 - \frac{1}{4}\alpha_2 \omega a_1^3 + \frac{3}{8}\alpha_3 \omega a_1^3 - \frac{\omega_c}{2a_1\gamma_2\omega}\gamma_1 a_2^2 \sigma_2 + \frac{\omega_c}{2a_1\gamma_2\omega}\gamma_1 a_2^2 \sigma_1 \quad (31.b)$$

$$\frac{a_1}{4\omega_c}\gamma_2 \sin\phi_2 = -\frac{1}{2}\mu \quad (31.c)$$

$$\frac{a_1}{4\omega_c}\gamma_2 \cos\phi_2 = \frac{\sigma_2}{2} - \frac{\sigma_1}{2} \quad (31.d)$$

The beam's and controller's frequency response equations can be derived from Equations (31) which takes the following form:

$$(\frac{f_1}{2\omega})^2 = (-a_1\sigma_1 - \frac{1}{4}\alpha_2\omega a_1^3 + \frac{3}{8}\alpha_3\omega a_1^3 - \frac{\omega_c}{2a_1\gamma_2\omega}\gamma_1 a_2^2\sigma_2 + \frac{\omega_c}{2a_1\gamma_2\omega}\gamma_1 a_2^2\sigma_1)^2 + (\frac{1}{2}ca_1 + \frac{\omega_c}{2\omega\gamma_2 a_1}\gamma_1\mu a_2^2)^2 \quad (32)$$

$$(\frac{1}{4\omega_c}\gamma_2 a_1)^2 = (\frac{1}{2}\mu)^2 + (-\frac{\sigma_1}{2} + \frac{\sigma_2}{2})^2 \quad (33)$$

A Jacobian matrix is derived from Equations (30) to assess the stability of the steady-state solutions using the resultant matrix's eigenvalues. This can be done by letting that

$a_n = a_{n0} + a_{n1}$ and $\phi_n = \phi_{n0} + \phi_{n1}$ (34)

where a_{n0} and ϕ_{n0} satisfy Eqs. (31), while a_{n1} and ϕ_{n1} are small-valued quantities compared to a_{n0} andϕ_{n0}. Substituting Equations (34) into (31) with linearizing the terms containing a_{n1} and ϕ_{n1} lead to

$$\begin{bmatrix} \dot{a}_{11} \\ \dot{\phi}_{11} \\ \dot{a}_{21} \\ \dot{\phi}_{21} \end{bmatrix} = [J] \begin{bmatrix} a_{11} \\ \phi_{11} \\ a_{21} \\ \phi_{21} \end{bmatrix} \quad (35)$$

where $J = \begin{pmatrix} u_{11} & u_{12} & u_{13} & u_{14} \\ u_{21} & u_{22} & u_{23} & u_{24} \\ u_{31} & u_{32} & u_{33} & u_{34} \\ u_{41} & u_{42} & u_{43} & u_{44} \end{pmatrix}$ and its entries are given in the Appendix. The Jacobian matrix's characteristic equation is

$$q^4 + \delta_1 q^3 + \delta_2 q^2 + \delta_3 q + \delta_4 = 0 \quad (36)$$

where q denotes the eigenvalue and $\delta_1, \delta_2, \delta_3, \delta_4$ are given in the Appendix. Accordingly, if all the real parts of q are negative, then the steady-state solution is stable. Otherwise, it is unstable. In addition, the necessary and sufficient criteria, according to Ruth-Hurwitz criterion, for all the roots in Equation (36), to have negative real parts are

$\delta_1 > 0$, $\delta_1\delta_2 - \delta_3 > 0$, $\delta_3(\delta_1\delta_2 - \delta_3) - \delta_1^2\delta_4 > 0$, $\delta_4 > 0$ (37)

IV. GRAPHICAL ANALYSIS ON THE CANTILEVER BEAM'S MOTION

In this section, the selected values for the beam and controller parameters are chosen as: $\omega = 0.5$, $\sigma_2 = 0$, $\alpha_1 = -0.0694$, $\alpha_2 = 4.5967$, $\alpha_3 = 3.2712$, $\omega_c = 0.25$, $\gamma = 0.1$, $c = 0.011$, $F = -0.001$, $\bar{F} = 0.1$, $\Omega_1 = 0.5$, unless otherwise stated. The relationship between the cantilever beam's amplitude of response a and the detuning value σ_1 before and after NSC control is illustrated by the graphical curves from 2 to 4. The stable solutions are shown by black lines on these curves, whereas the unstable solutions are represented by light lines. The frequency-response curves of the controller and the primary system with different stimulating forces f_1 are displayed in Figure (2).

In Figure (2a), the steady-state amplitude of the main system is a function that grows monotonically based on the amplitude of the excitation force. The jump phenomenon appears because of the dominance of the nonlinearity, and the curve is bent to the right as the force amplitude increases, denoting a hardening effect. The equilibrium amplitudes of the beam and NSC, in Figures (2b) and (2c), are directly proportional to the exciting force amplitude f_1. When $f_1 = 0.001$, the amplitude is stable Through the interval $-0.07 < \sigma_1 < 0.07$. NSC is approximately between the two values $\sigma_1 = \pm 0.07$, and the beam's steady-state amplitude is at its lowest level at $\sigma_1 = 0$. Also, the jump phenomena appear obviously for the NSC and the beam as depicted by the curve

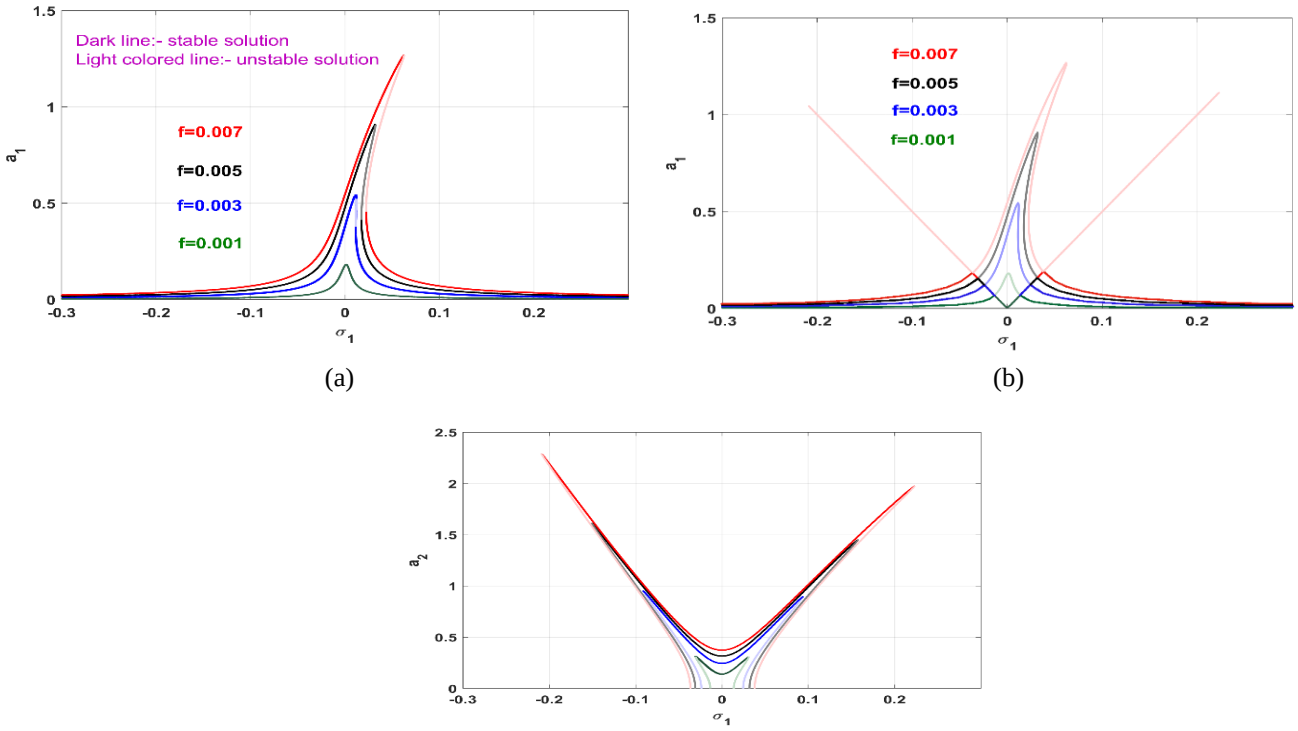

(a) (b)

(c)

Figure 2. Frequency-response curves pre and post NSC control: (a) beam's amplitude pre-control, (b) beam's amplitude post-control, (c) NSC's amplitude.

Figure (3) displays the frequency-response curves of the beam after NSC with different gain parameters $\gamma_1 = \gamma_2$. In Figure (3a) and (3b), when gain increased, the bandwidth increased, the amplitude decreased and nears to zero so this controller is suitable for this beam. When the vibration amplitude decreases, the system is more stable.

Figure (4) displays the frequency-response curves of the beam after NSC with different μ parameter at $\gamma_1 = \gamma_2 = 0.1$ and $f_1 = 0.005$. In Figure (4a), when μ decreased, the bandwidth increased and the amplitude decreased and nears to zero.

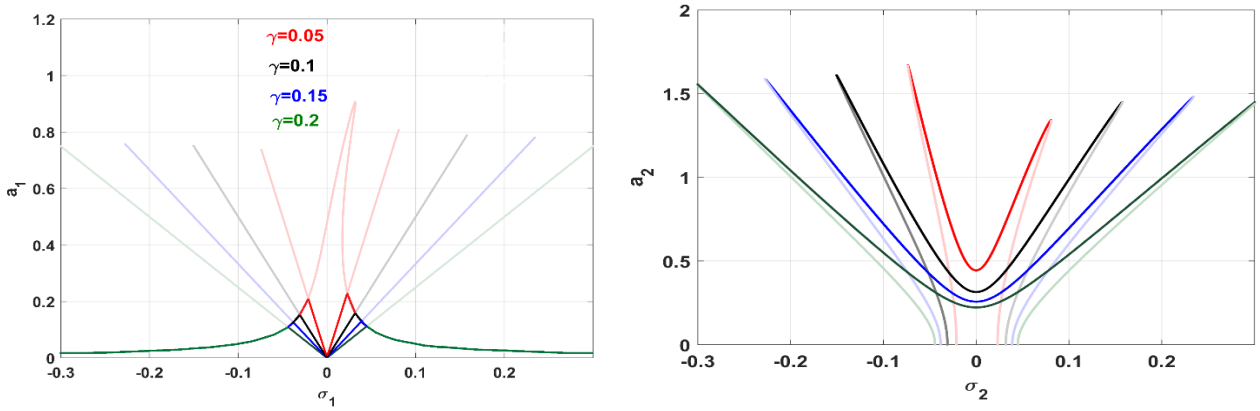

(a) (b)

Figure 3. Frequency-response curves after NSC control at $f_1 = 0.005, \mu = 0.001$: (a) beam's amplitude pre-control, (b) NSC's amplitude.

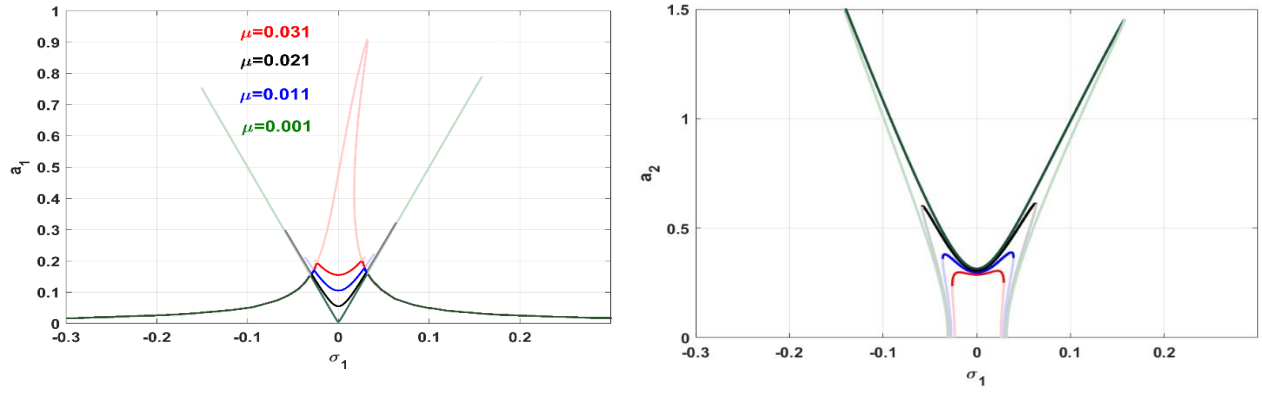

(a) (b)

Figure 4. Frequency-response curves after NSC control at $f_1 = 0.005, \gamma_1 = \gamma_2 = 0.1$: (a) beam's amplitude with control, (b) NSC's amplitude.

Figure (5) depicts the force response curve, which illustrates the relationship between force and amplitude before and after NSC control $\mu = 0.001, \gamma_1 = \gamma_2 = 0.1$with varying detuning parameters. When force increases in Fig. 5a at $\sigma_1 = 0$, the amplitude also increases and becomes more unstable. There are jump phenomena in this curve. The beam is more steady when we apply the saturation control shown in Figure (5b). It is preferable to use a cantilever beam system when the detuning parameter is equal to zero, which results in zero beam amplitude.

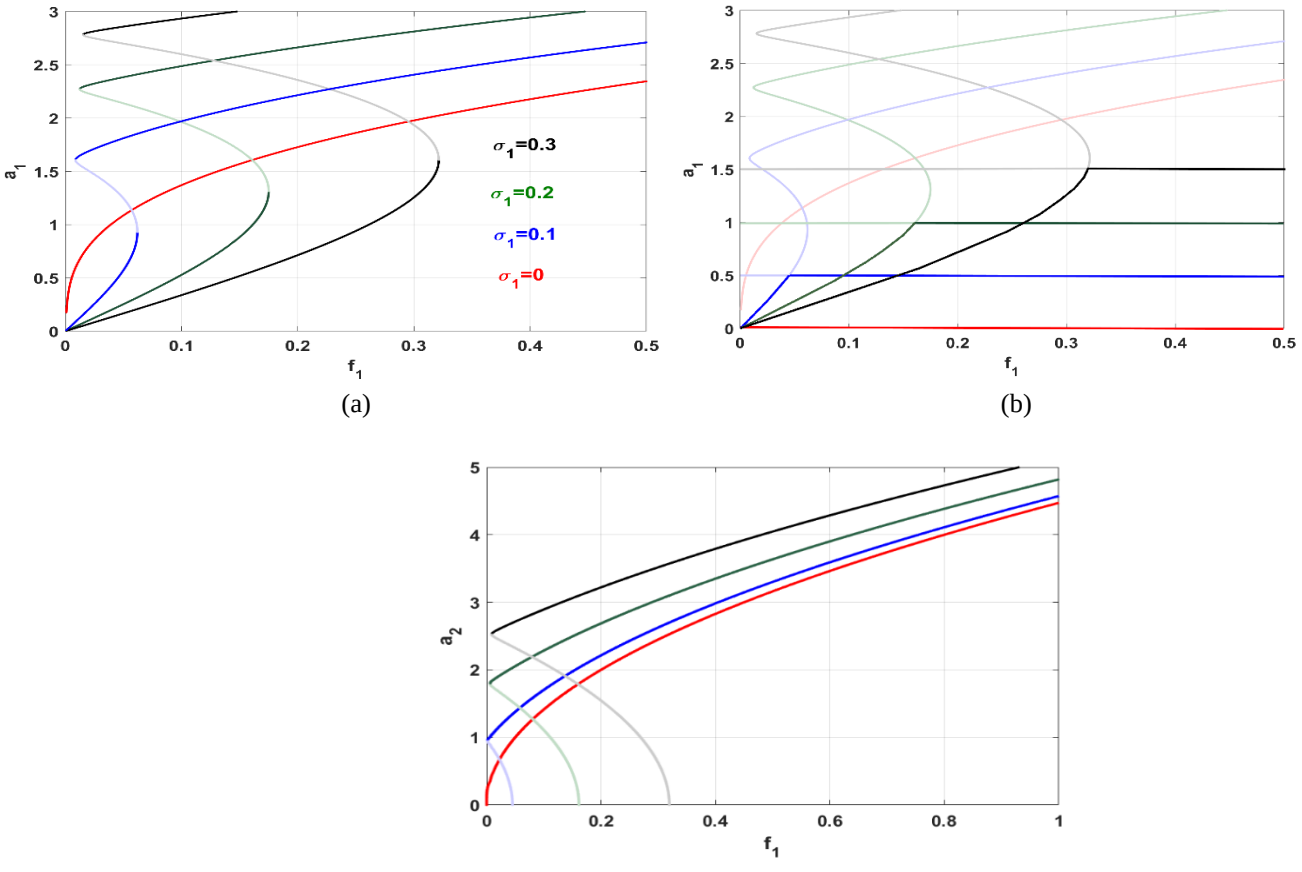

(a) (b)

(c)

Fig. 5 Force-response curves pre and post NSC control: (a) beam's amplitude pre-control, (b) beam's amplitude post-control, (c) NSC's amplitude.

Time history of the equilibrium amplitude of the uncontrolled and controlled beam near the simultanous resonance case $\Omega = \omega + \sigma_1$ and $2\omega_c = \omega + \sigma_2$ are numerically simulated as shown in Figures (6) to (7) using ODE45 tool in the MATLAB software. At $f_1 = 0.005$ and $(\sigma_1 = \sigma_2 = 0)$ according to Figure (6a), the beam's uncontrolled amplitude is approximately 0.347, while the controlled beam's amplitude is around 0.035. According to the phase portraits of Figures (6b) and (6d), the uncontrolled beam, the controlled beam, and the NSC all have stable steady-state amplitudes.

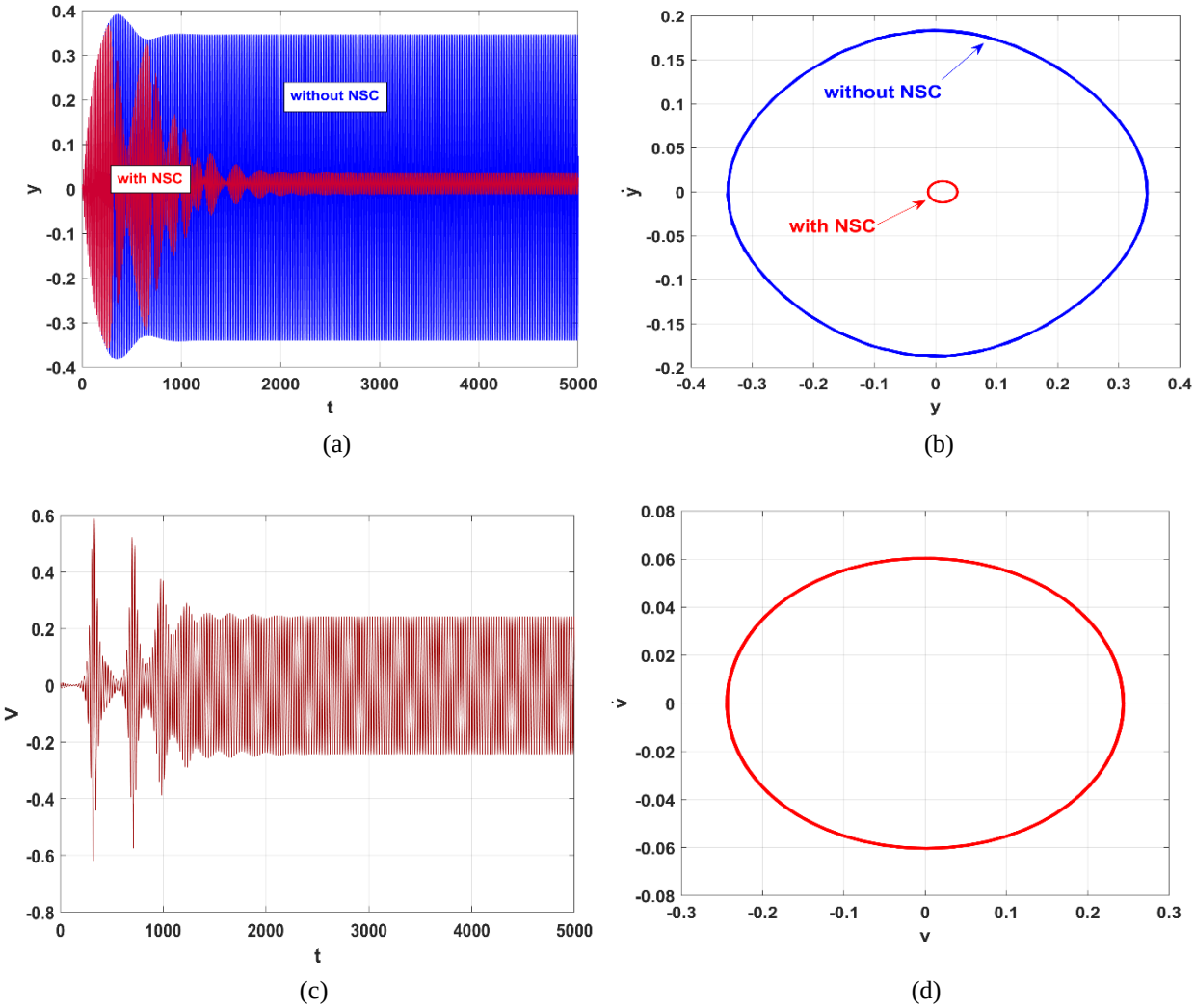

Fig. 6 The cantilever beam's time-vibrations before and after control for $f_1 = 0.003$: (a) the beam's time response and phase plane before control; (b) the beam's time response and phase plane after control; (c, d) time reponse and phase plane of the NSC.

At $f_1 = 0.004$ and $(\sigma_1 = 0.01, \sigma_2 = 0)$ according to Figure (7a), the uncontrolled beam has an unstable amplitude becouse time increases, the amplitude of beam becames unstable, whereas the controlled beam has an amplitude that tends to about zero and is approximately 0.068. According to the phase plane of Figures (7b), and (7d), the steady-state amplitude of the NSC is stable and amplitude of beam is unstable.

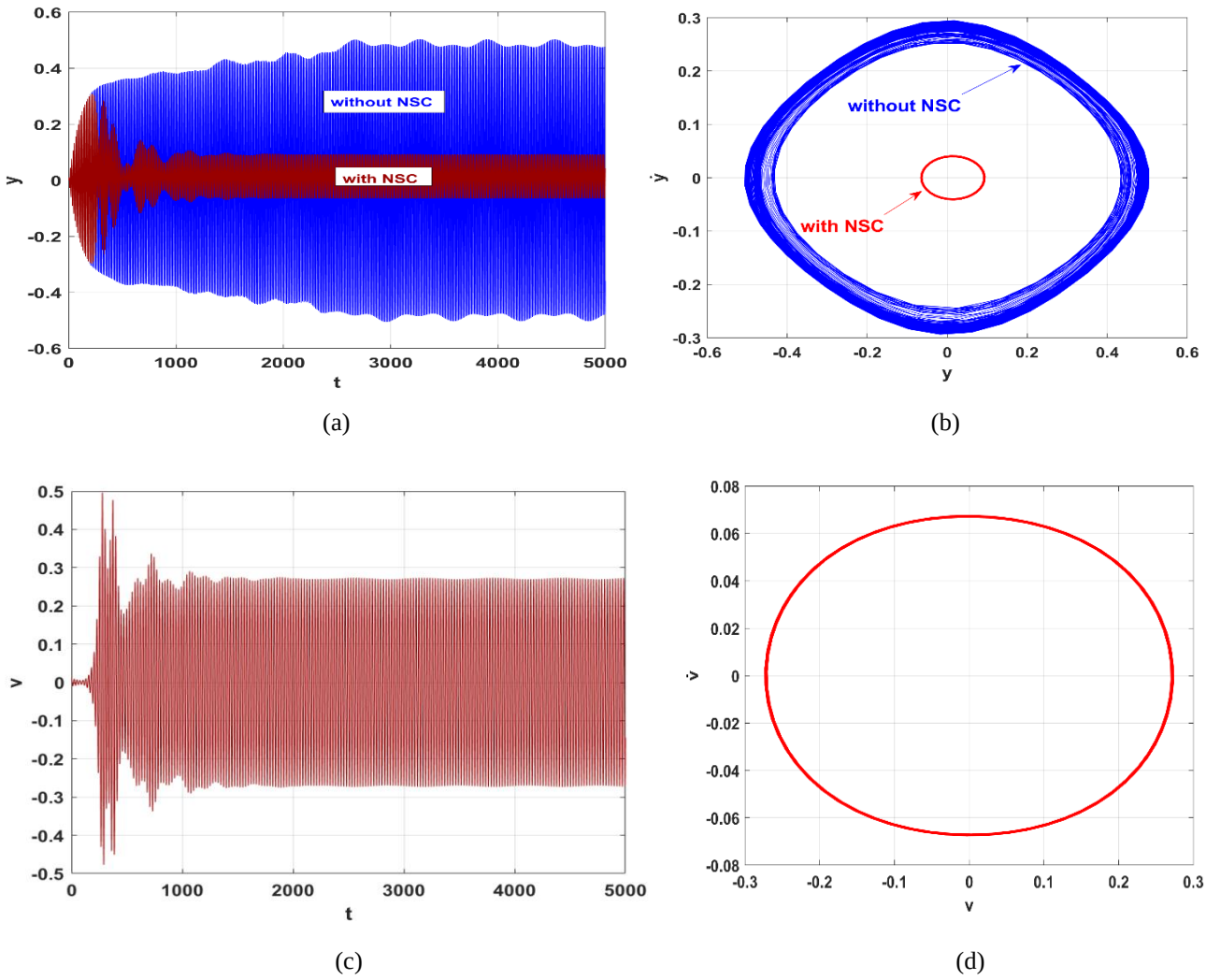

Fig. 7 The cantilever beam's time-vibrations before and after control for $f_1 = 0.004$:(a) the beam's time response and phase plane before control; (b) the beam's time response and phase plane after control; (c, d) time response and phase plane of the NSC.

V. CONCLUSION

In this paper, the nonlinear oscillations of a parametrically excited dynamical cantilever beam were analyzed and controlled. Within this model, we implemented NSC algorithm and retrieved the equation's analysis before and after control. There were multiple responses that demonstrated the dynamic behavior under control. Ultimately, we made a comparison between the numerical and analytical results obtained before and after control. The following points can be used to summarize these findings:

1. The cantilever beam was suffering from high-amplitude vibrations and jump phenomena in some conditions.
2. After control, the beam's vibrations reached the lowest level at $\sigma_1 = 0$ and quite lower levels within the range $\sigma_1 \in [-0.03, 0.03]$.
3. To increase the bandwidth of small amplitudes, the control gain was raised for enhancing this purpose.
4. Reducing the controller's damping μ could help in keeping the beam's vibrations at its minimum level when $\sigma_1 = 0$.
5. The beam's vibration amplitude was saturated at specific values even if the external force amplitude increased.

APPENDIX

The entries of the Jacobian matrix J in Equation (35):

$$u_{11} = -\frac{1}{2}c$$

$$u_{12} = \frac{f_1}{2\omega}\cos\phi_1$$

$$u_{13} = \frac{a_2}{2\omega}\gamma_1 \sin\phi_2$$

$$u_{14}=\frac{a_2^2}{4\omega}\gamma_1\cos\phi_2,$$

$$u_{21}=\frac{1}{2}\alpha_2\omega a_1-\frac{3}{4}\alpha_3\omega a_1-\frac{f_1}{2\omega a_1^2}\cos\phi_1 -\frac{a_2^2}{4\omega a_1^2}\gamma_1\cos\phi_2$$

$$u_{22}=-\frac{f_1}{2\omega a_1}\sin\phi_1$$

$$u_{23}=\frac{a_2}{2\omega a_1}\gamma_1\cos\phi_2$$

$$u_{24}=-\frac{a_2^2}{4\omega a_1}\gamma_1\sin\phi_2$$

$$u_{31}=-\frac{a_2}{4\omega_c}\gamma_2\sin\phi_2$$

$$u_{32}=0$$

$$u_{33}=-\frac{1}{2}\mu-\frac{a_1}{4\omega_c}\gamma_2\sin\phi_2$$

$$u_{34}=-\frac{a_1a_2}{4\omega_c}\gamma_2\cos\phi_2$$

The coefficients of Equation (36):

$$\delta_1=-u_{11}-u_{22}-u_{33}-u_{44}$$

$$\delta_2=-u_{12}u_{21}+u_{11}u_{22}+u_{33}u_{11}+u_{11}u_{44}+u_{33}u_{22} +u_{44}u_{22}-u_{34}u_{43}-u_{42}u_{24}-u_{23}u_{32}-u_{13}u_{31} -u_{14}u_{42}-u_{14}u_{41}$$

$$\delta_3=-u_{11}u_{33}u_{22}-u_{11}u_{44}u_{22}+u_{11}u_{34}u_{43}-u_{33}u_{44}u_{22} -u_{11}u_{42}u_{24}-u_{22}u_{33}u_{44}+u_{34}u_{43}u_{22}+u_{11}u_{23}u_{32} +u_{23}u_{32}u_{44}-u_{23}u_{34}u_{42}-u_{24}u_{32}u_{43}+u_{24}u_{33}u_{42} +u_{12}u_{21}u_{33}+u_{12}u_{21}u_{44}-u_{12}u_{23}u_{31}-u_{12}u_{24}u_{41} -u_{13}u_{32}u_{21}+u_{13}u_{22}u_{31}+u_{13}u_{31}u_{44}-u_{13}u_{34}u_{41} -u_{14}u_{21}u_{42}+u_{14}u_{22}u_{42}-u_{14}u_{31}u_{43}+u_{14}u_{42}u_{33}$$

$$\delta_4=u_{11}u_{22}u_{33}u_{44}-u_{11}u_{34}u_{43}u_{22}-u_{11}u_{23}u_{32}u_{44}-u_{11}u_{23}u_{34}u_{42} -u_{11}u_{24}u_{32}u_{43}-u_{11}u_{24}u_{33}u_{42}-u_{12}u_{21}u_{33}u_{44}+u_{12}u_{21}u_{34}u_{43} +u_{12}u_{23}u_{31}u_{44}-u_{12}u_{23}u_{34}u_{41}-u_{12}u_{24}u_{31}u_{43}+u_{12}u_{24}u_{41}u_{33} +u_{13}u_{21}u_{32}u_{44}-u_{13}u_{21}u_{34}u_{42}-u_{13}u_{22}u_{31}u_{44}+u_{13}u_{22}u_{34}u_{41} +u_{13}u_{24}u_{31}u_{42}-u_{13}u_{24}u_{32}u_{41}-u_{14}u_{21}u_{32}u_{43}+u_{14}u_{21}u_{42}u_{33} +u_{14}u_{22}u_{31}u_{43}-u_{14}u_{22}u_{42}u_{33}-u_{14}u_{23}u_{31}u_{42}+u_{14}u_{23}u_{32}u_{41}$$

REFERENCES

[1] N. Herisanu and V. Marinca, "Explicit analytical approximation to large-amplitude non-linear oscillations of a uniform cantilever beam carrying an intermediate lumped mass and rotary inertia," Meccanica Journal, 45(6):847–855, 2010.

[2] Y. H. Qian, S.K. Lai, W. Zhang and Y. Xiang, "Study on asymptotic analytical solutions using HAM for strongly nonlinear vibrations of a restrained cantilever beam with an intermediate lumped mass," Journal of Numerical Algorithms, 58(3): 293-314, 2011.

[3] A. Nikkar, S. Bagheri and M. Saravi, "Dynamic model of large amplitude vibration of a uniform cantilever Beam carrying an intermediate lumped mass and rotary inertia," Latin American Journal of Solids and Structures, 11: 320–329, 2014.

[4] B. Pratiher and S.K. Dwivedy, 'Nonlinear vibrations and frequency response analysis of a cantilever beam Under periodically varying magnetic field," Mech. Based Des. Struct. Mach. 39, 378–39, 2011.

[5] M. Sadri, D. Younesian and E. Esmailzadeh, "Nonlinear harmonic vibration and stability analysis of a cantilever beam carrying an intermediate lumped mass," Nonlinear Dynamics, 84:1667-1682, 2016.

[6] A. Kumar, "Effect of approximation of curvature/inertia on the nonlinear vibrations of cantilever beam Structures," 26, 737–744, 2020.

[7] V. Ondra and B. Titurus, "Free vibration and stability analysis of a cantilever beam axially loaded by an Intermittently attached tendon," Mech. Syst. Signal Process. 158, 2021.

[8] W. Zhang, "Chaotic motion and its control for nonlinear nonplanar oscillations of a parametrically excited cantilever beam. Chaos," Solitons and Fractals. 26, 731–745, 2005.

[9] M. Sayed, A. A. Mousa, D. Y. Alzaharani, I. H. Mustafa, and S. I. El-Bendary, "Bifurcation analysis of a composite cantilever beam via 1:3 internal resonance," Journal of the Egyptian Mathematical Society. September, 2020.

[10] O. M. Omara, M. Sayed, and N. A. Saeed, "Vibration control of a horizontally supported Jeffcott-rotor system utilizing PIRC-controller," Menoufia Journal of Electronic Engineering Research (MJEER), VOL. 32, NO. 2, July, 2023.

[11] S. Subhashini and A. Juliet, "Toxic gas sensor using resonant frequency variation in micro-cantilever," Sustainable Utilization and Development in Engineering and Technology, IEEE Conference, 87-91, 2012.

[12] M. S. Hanay, S. Kelber, A. K. Naik, D.Chi, S. Hentz, E. C. Bullard, E. Colinet, L. Duraffourg and M. L. Roukes, "Single-protein nano mechanical mass spectrometry in real time," Nature Nanotechnology, 7: 602-608, 2012.

[13] A. Ramini, K. Masri, and M. Younis, "Electrostatically actuated resonant switches for earthquake detection," Mechatronics and its Applications (ISMA), 9th International Symposium, 1-7, 2013.

[14] J. Rhoads, V. Kumar, S. Shaw and K. Turner, "The nonlinear dynamics of electromagnetically actuated micro beam resonators with purely parametric excitations," International Journal of Non-Linear Mechanics, 55: 79-89, 2013.

[15] J. Przybylski and G. Gasiorski, "Nonlinear vibrations of elastic beam with piezoelectric actuators," Journal of Sound and Vibration, 437(2):150-165, 2018.

[16] J. Latalski and J. Warminski, "Nonlinear vibrations of a rotating thin-walled composite piezo-beam with circumferentially uniform stiffness (CUS)," Nonlinear Dynamics, 98: 2509 – 2529, 2019.

[17] F. Ebrahimi, S. Hamed and S. Hosseini, "Nonlinear dynamic modeling of smart graphene/piezoelectric composite nanoplates subjected to dual frequency excitation," Engineering Research Express, 2(2):025019, 2022.

[18] J. Tuma, "Analysis of active vibration control for a cantilever beam with the use of the lumped parameter model," Dynamic of machines 2012. February 7-8, Prague, Cyech Republic, 157-164, 2012.

[19] M. Kamel, A. Kandil, W.A. El-Ganaini and M. Eissa, "Active vibration control of a nonlinear magnetic levitation system via nonlinear saturation controller (NSC)," 605–619, Aug, 2014.

[20] M. Eissa, A. Kandil, W.A. El-Ganaini and M. Kamel, "Vibration suppression of a nonlinear magnetic levitation system via time delayed nonlinear saturation controller," 23–41, Jun, 2015.

[21] A. Kandil and H. A. El-Gohary, ''Suppressing the nonlinear vibrations of a compressor blade via a nonlinear saturation controller," 1488–1504, Apr. 2018.

[22] F. R. Zemtchou, J. S. Takam, P. N. Nguenang and P. K. Talla, "Amplitude resonance response and feedback control of cantilever beams with tip-mass under aerodynamic load," Journal of Physica Scripta, 12:125271, 2021.

[23] Y. S. Hamed and A. Kandil, "Influence of time delay on controlling the non-linear oscillations of a rotating blade," Symmetry, vol. 13, pp. 1–18, Jan. 2021.

[24] C. Liu, Y. Yan and W. Wang, "primary and secondary resonance analyses of a cantilever a beam carrying an intermediate lumped mass with time-delay feedback," Nonlinear Dynamics, 97:1175-1195, 2019.

[25] Y.S. Hamed, A. El Shehry and M. Sayed, "Nonlinear modified positive position feedback control of cantilever beam system carrying an intermediate lumped mass," Alexandria Engineering Journal, 59:3847-3862, 2020.

[26] Y. A. Amer, A. T. EL-Sayed and M. N. Abd EL-Salam, "A Suitable Active Control for Suppression the Vibrations of a Cantilever Beam," Journal of sound & vibration, 2022.

[27] A. H. Nayfeh, "Nonlinear Interactions," Jon Wiley & Sons, Inc., New York, 2000.

[28] A. H. Nayfeh and D. T. Mook, "Nonlinear Oscillations," Wiley Interscience, New York, 2004.